A new PCM-TRC composite: A mechanical and physicochemical investigation

Zakaria Ilyes Djamai, Amir Si Larbi, Ferdinando Salvatore, Gaochuang Cai

A new PCM-TRC composite: a mechanical and physicochemical investigation

Zakaria Ilyes Djamai[1], Amir Si Larbi[2], Ferdinando Salvatore[2], Gaochuang Cai[2]

1-LMDC (Laboratoire Matériaux et Durabilité des Constructions), Université de Toulouse, INSA/UPS Génie Civil, 135 Avenue de Rangueil, 31077 Toulouse cedex 04, France.

2-Université de Lyon, Ecole Nationale d'Ingénieurs de Saint-Etienne (ENISE), Laboratoire de Tribologie et de Dynamique des Systèmes (LTDS), 58 Rue Jean Parot, 42000 Saint-Etienne, France

Corresponding author: djamai@insa-toulouse.fr

Abstract

The present paper presents a multiscale and multiphysics study that focuses on the development of an innovative composite material, which combines a cementitious matrix modified by a phase-change material (PCM) with textile reinforcement (PCM-TRC).

The development of this composite has been guided by the conjunction of several factors, among which it is appropriate to emphasise the lightweight of the composite due to the reduced covers in textile reinforced concrete (TRC) coupled to the high thermal inertia due to the addition of PCM microcapsules.

This research focuses on the effect of PCM on the mechanical and physicochemical properties of TRC. Special emphasis is placed on providing the phenomenological explanation for the resulting mechanical behaviour of TRC according to the rate and state of the PCM.

It has been found that the ductile mechanical behaviour of TRC composites is maintained in the presence of microencapsulated PCM; however, the mechanical performance of PCM-TRC decreases with the PCM rate. This is due to the disorder caused by PCM at the matrix and interface scales. Furthermore, it has been found that the PCM state (solid or liquid) can affect the mechanical performance of both the PCM–mortar matrix and PCM-TRC composite. This is due to PCM expansion during phase change from the solid to the liquid state, which can induce matrix microcracking.

Key words

PCM, TRC, composite material, mechanical behaviour, physicochemical investigation.

1-Introduction

The building sector has a strong potential for improvement in terms of thermal performance and reduction of its ecological footprint. In this context, composite structures and non-conventional materials are widely used.

Textile-reinforced concrete (TRC) consists of a fine-grained concrete matrix reinforced with alkali-resistant glass fabric, basalt, aramid… [1, 2]. TRC combines the high compressive strength of a cementitious matrix with the high tensile resistance of a non-corrosive textile fabric and thus allows the construction of lightweight cementitious elements, such as lightweight roofs, sandwich

panels, etc. [3, 4, 5, 6]. TRC can ensure fire resistance and constitutes an important alternative to fibre-reinforced polymer, which has limitations in terms of cost, fire resistance, toxicity, and sustainable-development features attributed to the polymer matrix [6]. Despite these advantages, the light weight of TRC, which is due to the low thickness of the concrete covers, can lead **to a considerable reduction of its thermal inertia**.

Recent studies [7, 8, 9] have focused on the search for intelligent materials that have the ability to regulate indoor temperature variations; these are phase-change materials (PCMs). PCMs change their phase from solid to liquid in warm periods by storing heat, the same heat that is released in cold periods, when the PCM returns to the solid state. This repetitive energy storage–release process can smooth out temperature variations inside buildings when PCMs are integrated in the materials constituting the building envelope.

The most promising association is probably the direct integration of PCMs in cement-type materials, which are the most commonly used in construction. Recent studies have identified several techniques for integrating PCMs into cementitious materials, such as direct incorporation of raw PCMs [10] and vacuum impregnation in cementitious materials [11]. However, the technique that has received the most attention from the scientific community is the integration of PCMs after microencapsulation [12,13]. This method allows coating the raw PCM with a polymer film in the form of a capsule, which makes it possible to protect the PCM from a possible liquid-phase flow and thus potential mixing with the cementitious components (whose effects are not controlled).

Recent investigations [14, 15] have shown that the integration of microencapsulated PCM in cementitious materials can considerably improve their energy storage capacity; however, this is combined with an important degradation of their mechanical performance [16, 17, 18, 19, 20].

In this context, the present study aims to combine the advantages of PCM and TRC to propose **a new PCM-modified TRC composite, PCM-TRC,** which results from the association of a PCM-modified mortar matrix and an alkali-resistant glass fabric reinforcement. The main advantages of the new PCM-TRC composite material can be summarised as follows:

a) The possibility to produce lightweight cementitious structural elements (**owing to TRC**) with high mechanical performances (especially under tension solicitation) and high thermal inertia (**owing to PCM**).

b) It is a better match (even partial) to the criteria of sustainable development.

Few studies have focused on the effect of PCM on the mechanical performances of fibrous reinforced concrete and TRC. Savija et al. [21] studied the effect of PCM on the strength of PVA fibrous reinforced mortar. They concluded that the addition of small amounts of microencapsulated PCMs can be detrimental to compressive strength, although it has a small effect on flexural strength and deflection capacity.

For all these reasons, the main objective of this research is to **investigate whether PCM affects the mechanical properties of TRC**, especially regarding the tensile response of the composite. This study **also focuses on the physicochemical explanation** of the resulting changes in the mechanical strength of the composite due to the PCM rate.

Furthermore, few studies [22] have focused on how the state of microencapsulated PCM (solid or liquid) influences the mechanical characteristics of PCM–cementitious materials. For this reason, this research analyses the effects of the temperature (and thus of the PCM state) on the mechanical performances of PCM–mortar matrices and its consequences on PCM-TRC composites. Phenomenological explanations of such changes due to the PCM state are also provided in the paper.

Recent studies [23] on the life cycle assessment (LCA) of PCM-concrete constructions, point out the need of research to reduce the environmental impact of using PCM in construction. In fact, these investigations indicate that the energy saving achieved during the operational phase of PCM-concrete constructions is balanced out with the manufacturing and end of life phases of raw PCM, which is generally derived from petroleum resources like paraffin. For this reason, the present research aims also, to compensate or at least reduce the negative effect of the manufacturing phase of PCM in LCA using a natural vegetal wax, which is a fatty ester, identified as methylexadecanoate in the PCM-TRC composites. In fact, recent researchers [23] pointed out that the use of hydrated salts and natural fatty esters can present a 75% lower manufacturing environmental impact than paraffin.

2-Material and methods

2-1 Materials

2-1-1 Mortar

A Portland cement mortar with fine aggregate (D<1.6 mm) was chosen to ensure the impregnation of the textile fabric for the 'PCM-TRC' composites.

2-1-2 PCM

The PCM used in the study is a non-paraffinic fatty ester vegetal wax chemically identified as methylexadecanoate; this PCM was selected to minimise the environmental impact. The PCM phase-change temperature ranges from 24 to 27°C with a phase-change peak at 25°C. The latent heat of the phase change of PCM is 160 kJ/kg. The differential scanning calorimetry (DSC) diagram for one endothermic cycle of the PCM is provided in [12].

2-1-3 Textile fabric reinforcement

The textile fabric reinforcement used in the study is an alkali-resistant uncoated glass with a tensile yield stress and Young's modulus measured as 800±48 MPa and 53±2.5 GPa, respectively, and with a mesh width of 4 and 5 mm in the warp and weft directions, respectively.

2-2 Experimental methods

2-2-1 Casting procedure

2-2-1-1 Casting of the PCM-modified mortar matrix

Microencapsulated PCM was added to different weight percentages of Portland cement fine-grained mortar (0, 5, 10, and 15 wt%). A minimum of 5 wt% PCM is required to ensure a meaningful effect of the PCM in terms of thermal performance [24].

The specific nature of the encapsulated PCM [25, 26, 12, 19] induce two main phenomena. The first is water absoption in the internal porosity of PCM (the voids between microcapsules) due to its very high porosity and high surface specific area (~1000 m^2/kg). The second is water adsorption due to the existence of –OH groups on the polymer shell used for encapsulation, which lead to chemical water adsorption by creation of hydrogen bonds. The high hydrophilic nature of the encapsulated PCM require an adjustment of the water-to-binder ratio for each PCM–mortar matrix to **fulfil the requirement of equivalent workability that ensures equivalent conditions for the impregnation of the alkali-resistant (AR) glass textile fabrics in each PCM–mortar matrix.**

The amount of additional water required for each PCM–mortar matrix was evaluated using a water absorption test on PCM powder according to EN1097-6 [27]. The results are shown in **Table 1.**

Mass of surface dried (24h in 100°C oven) PCM powder M_1(g)	Mass of saturated PCM powder after 24h immersion M_2 (g)	Water absorption coefficient ($\frac{M_2-M1}{M1}$) in %
100	154	54

Table 1 Test results of water absorption capacity of PCM powder

The mix composition of the PCM-mortar matrix are presented **Table 2** [$\frac{w_1}{c}$ is the total water to cement ratio, $\frac{w_2}{c}$ is the ratio of water not absorbed by the PCM to cement, which is maintained constant in all the mix composition and leads to a quasi-constant slump (equivalent workability) in all the mix compositions (**see table 2**)].

The 40 mm × 40 mm × 160 mm specimens used for the mechanical tests on the PCM–mortar matrix at an age of 28 days were cast and cured under constant laboratory conditions (20°C).

PCM-mortars	Reference	5wt%	10wt%	15wt%
PCM (kg)	0	0.3	0.6	0.9
Cement (kg)	1.65	1.65	1.65	1.65
Fine aggregate(kg)	4.35	4.35	4.35	4.35
Water (L)	0.80	0.96	1.12	1.29
$\frac{w_1}{c}$	0.48	0.58	0.68	0.78

$\frac{w_2}{c}$	0.48	0.48	0.48	0.48
slump (mm)	182	185	178	179

Table 2 PCM-mortar mixture compositions

2-2-1-2 casting of the 'PCM-TRC' composites

The in situ hand lay-up technique (**Figure 1**) was applied to produce the PCM-TRC composites. A suitable amount of each PCM–mortar matrix (0, 5, 10, 15 and 20wt% PCM–mortar, as described above) was spread on the bottom of a mould (600 mm-length, 400 mm- width, 10 mm-thickness). Then, the AR glass fabric was impregnated by the matrix with a roller so that PCM–mortar matrix penetrated inside the textile fabric meshes. The procedure was repeated so that the PCM-TRC composites were reinforced with two layers of textile fabric. It should be emphasised that special care was taken to avoid damage to the PCM during the described process.

After casting, the samples were cut into 500 mm-length, 70 mm-wide, and 10 mm-thick specimens (making sure to eliminate curbs to avoid border effects) for mechanical evaluation under uniaxial tensile solicitation.

Figure 1 In-situ hand lay-up technique for PCM-TRC composites

2-2-2 Mechanical characterisation

2-2-2-1 Matrix scale: mechanical characterisation of the PCM-mortar matrix

Compression test, three-point bending test and stiffness analysis were realised on 40 mm × 40 mm × 160 mm specimens of the PCM–mortar matrices containing 0, 5, 10, and 15 wt% PCM at temperatures of 20°C and 40°C and an age of 28 days (five samples for each PCM content and at each temperature).

The specimens tested at 40°C were stored for 6 h in an oven at 45°C to induce PCM microcapsules phase change from the solid to the liquid state. Compression tests, three-points bending tests and stiffness analysis were performed 3 minutes after removal from the cold room.

Five specimens (of each PCM content) whose temperature was raised to 40°C were then cooled at 15°C for 6 hours in a cold room to ensure PCM re-solidification (sample surface temperature =

20°C). Compression tests, three-points bending tests and stiffness analysis were performed 3 minutes after removal from the cold room.

2-2-2-2 Matrix scale: explanation of the effect of temperature on the mechanical behaviour of PCM-mortar matrix.

The PCM state may affect the mechanical behaviour of both the PCM-mortar matrices and the PCM-TRC composites (see **section 3-1**).

The authors explored the hypothesis that a change occurs in the volume of the hardened PCM–mortar mixes, which is controlled by the PCM state (solid or liquid). Indeed, when PCM melts, the PCM capsule may expand, which can induce localised strains in PCM-mortar.

To evaluate the veracity of this hypothesis hardened PCM–mortar samples (40 mm × 40 mm × 160 mm) were first cooled to 15°C in a cold chamber to ensure solidification of all PCM in the hardened mortar. The samples containing 0, 5, 10, 15, and 20 wt% PCM were then instrumented before being placed in an oven at 45°C for 80 min (**Figure 2**).

The instrumentation of the samples in the oven (**Figure 2**) consisted of a strain gage (30 mm in length) placed on the front face of a PCM–mortar sample and a surface temperature sensor placed on a different face of the sample to correlate the strain evolution with the surface temperature of the sample. The two sensors (strain gage and surface temperature sensors) were connected to a data acquisition system. The PCM–mortar samples were then placed in a 45°C oven for approximately 80 min while the data acquisition system recorded the evolution of the axial strain and the surface temperature of the samples.

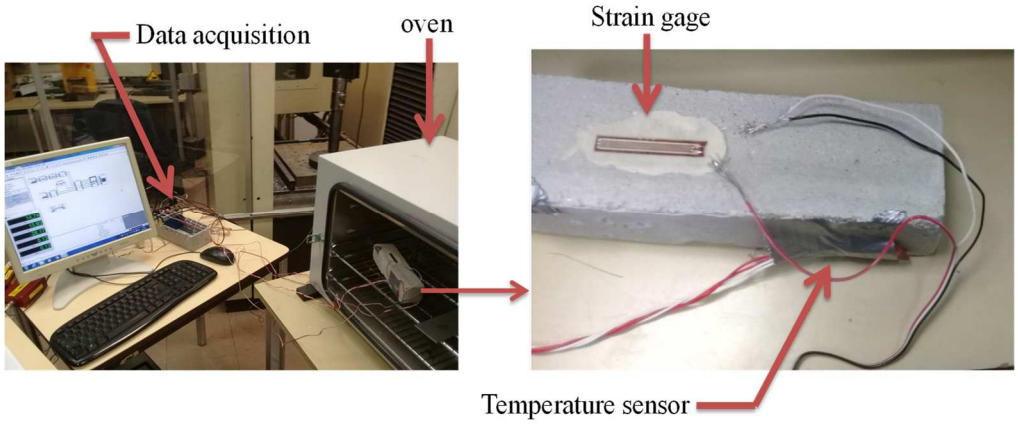

Figure 2 Experimental setup for investigating the effect of temperature

2-2-2-3 Composite scale: mechanical characterisation of PCM-TRC composites.

2-2-2-3-a Mechanical tests at variable PCM rate and constant temperature

Thin PCM-TRC specimens (500 mm-length, 70 mm-width, and 10 mm-thick) consisting of PCM–mortar matrix (0, 5, 10, 15 and 20wt% PCM) reinforced with two layers of AR glass fabric (which corresponds to a volume rate of reinforcement of 2.66% and 2.1 % in the warp and weft directions, respectively and a total fiber fraction volume of 4.76%) were tested under unidirectional tensile solicitation in the warp direction of the textile reinforcement (three

specimens for each PCM content) at an age of 28 days and at a **constant temperature of 20°C** (which means that PCM was in the solid state), according to the recommendation of the Rilem committee [28].

The tests were performed on an INSTRON electromechanical press with a capacity of 100 kN. The PCM-TRC specimens were clamped by applying a pressure of approximately 3 MPa to their upper and lower ends, while thin rubber plates (~2 mm thick) were glued on the grips to avoid any local compression crushing due to clamping. The clamping length was set to be 125 mm to avoid any local pull of the textile fabrics during the test.

During the test, the PCM-TRC specimens with 0, 5, 10, 15 and 20wt% PCM were instrumented with two LVDT sensors, one on each side of the sample (see **Figure 3**). The LVDT sensors measured the longitudinal displacement of the 200 mm central zone of the specimens.

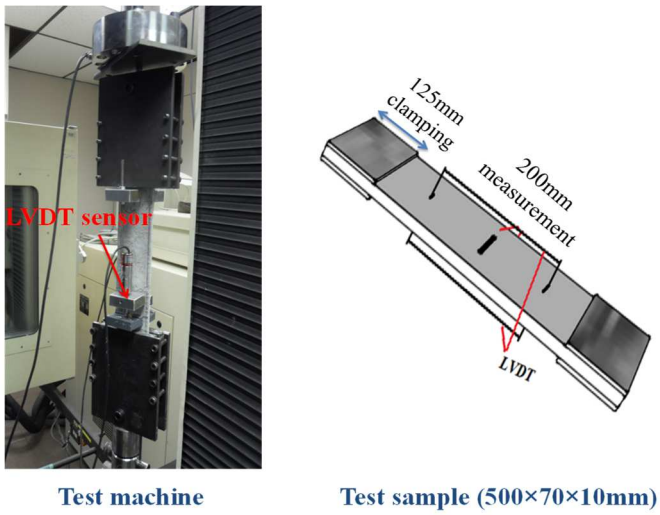

Figure 3 Tensile tests on PCM-TRC composites

2-2-2-3-b Mechanical tests at variable temperature and constant PCM rate

To analyse the effect of the temperature (and thus the PCM state) on the mechanical performance of PCM-TRC, the mechanical strength of the 10wt% PCM-TRC composite was evaluated in two different configurations (three specimens for each configuration):

-A- 10wt% PCM-TRC test specimens (500 mm × 70 mm × 10 mm) were maintained at a temperature of 20 °C and were then tested under tension at the same temperature.

-B- 10wt% PCM-TRC test specimens (500 mm × 70 mm × 10 mm) were initially kept at 20 °C and then placed in an oven at 40 °C for 6 h to induce phase change of the PCM (from solid to liquid). Three minutes after their removal from the oven, the specimens were tested under tension.

2-2-3 Physico-chemical characterisation of the PCM-TRC composites

2-2-3-1 SEM analysis

To better understand the effect of PCM on the mechanical behaviour of the PCM-TRC composites, SEM analyses of the matrix/textile interface were carried out on control TRC composites (without PCM) and on PCM-TRC composites with different PCM rates.

A TESCAN Mira3 FEG microscope with an electron voltage of 10 kV and a high-vacuum chamber with a pressure of 10^{-2} Pa were used for the SEM investigations. A backscattered electron detector (BSE) was used to identify the different phases existing in the composite.

2-2-3-2 DSC analysis

The specific heat capacity of PCM-TRC composites cured for 28 days was evaluated using a 3D CALVET scanning calorimeter, which contains an array of thermocouple sensors that totally surround the sample in the three directions and thus allow the introduction of approximately 2 g of hardened PCM-TRC composite (of each PCM rate) without crushing the material.

The heating range used for the endothermic test was 5–40°C with a heating rate of 2°C/min under low-vacuum pressure and a nitrogen purge (20 mL/min).

3-Results and discussion

3-1 mechanical characterisation

3-1-1 Mechanical characterisation of PCM-mortar matrices

Figure 4 (a, b and c) shows compression strength, bending strength and stiffness, respectively of PCM-mortar samples at 28days. The tests were performed on three types of samples: samples with temperatures maintained at 20°C; samples with temperatures raised to 40°C; and samples that were cooled to 20°C after having been heated to 40°C.

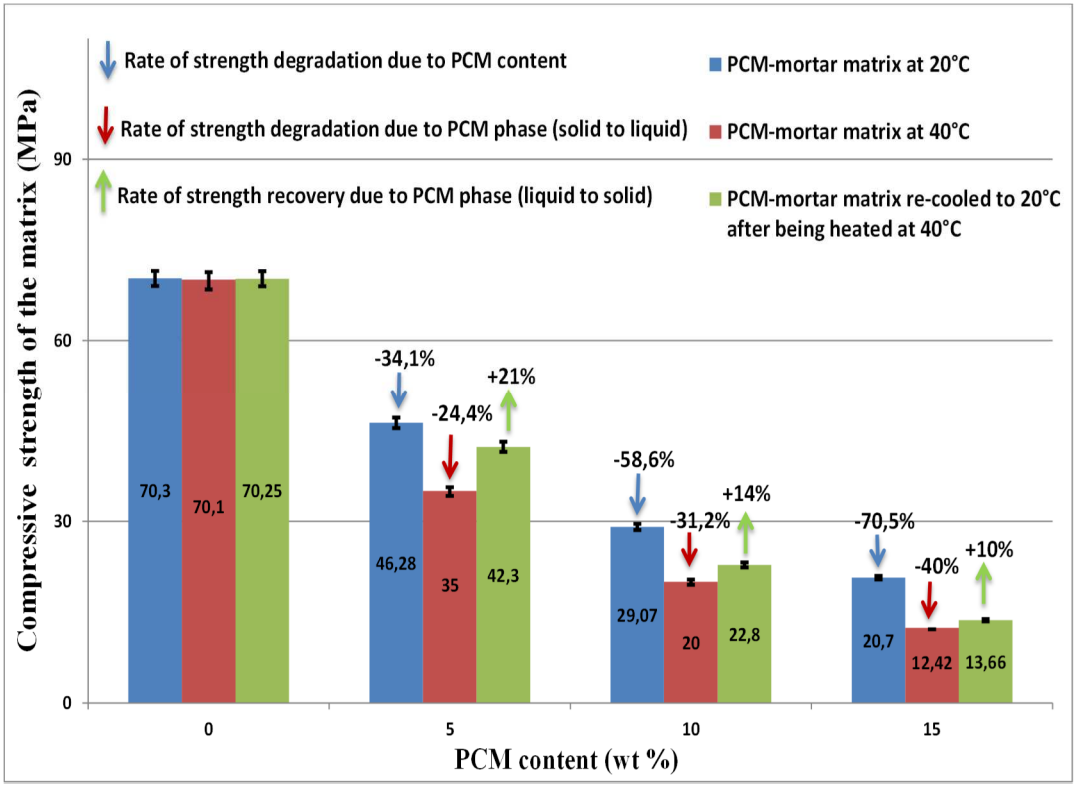

-a-

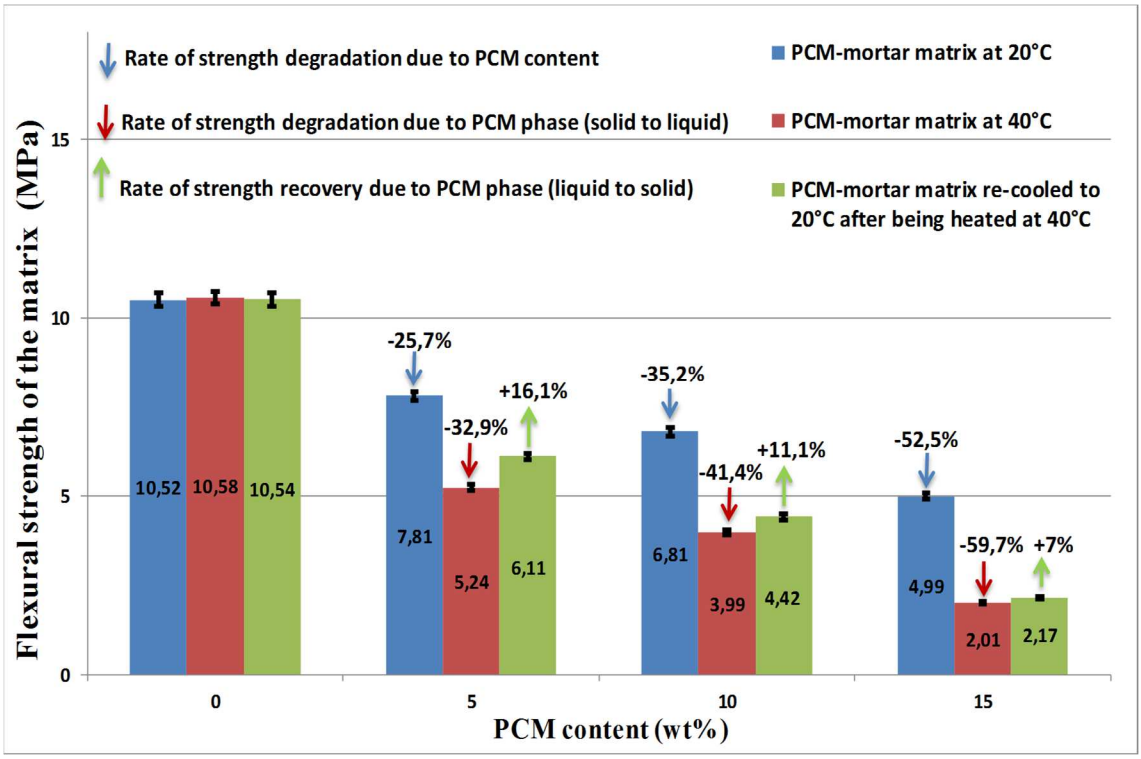

-b-

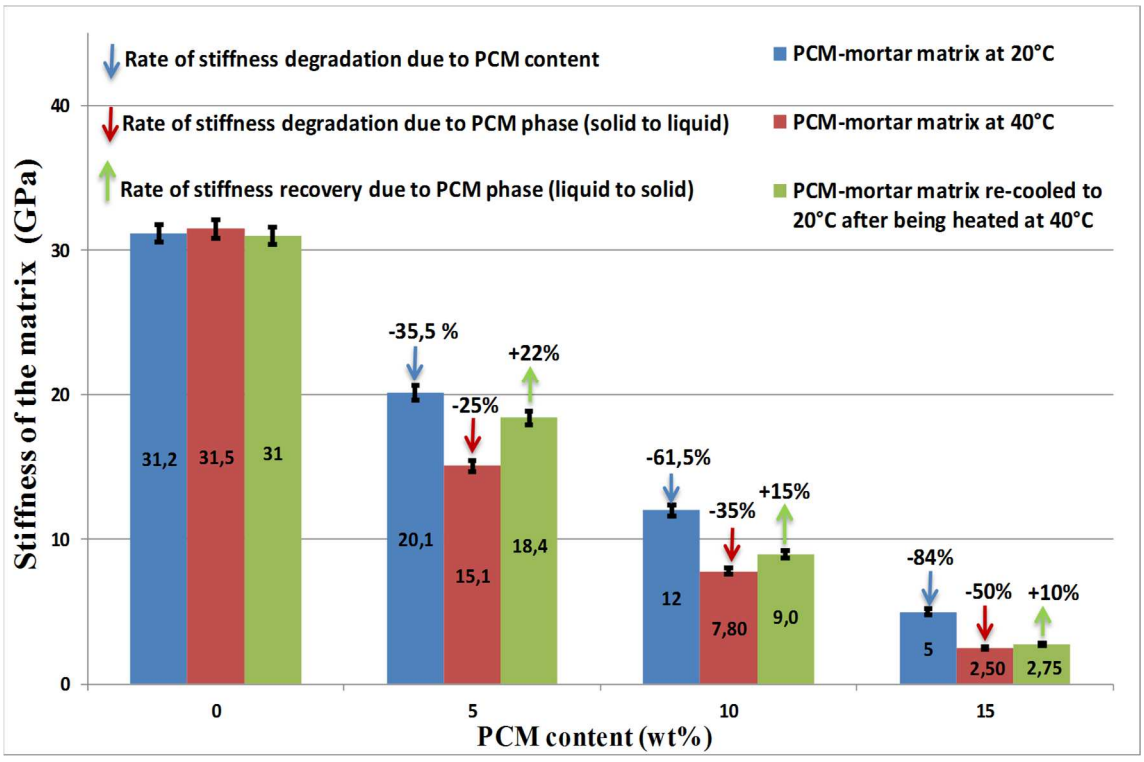

-c-

Figure 4 Effect of PCM rate and state on the (a) compressive strength, (b) flexural strength and (c) stiffness of the PCM-mortar matrix

The main results that can be derived from **Figure 4** can be summarised as follows:

(a) A decrease in the mechanical strength (under compression and flexion) and stiffness of the mortar was found for increasing PCM content in the three cases defined above (samples maintained at 20°C, samples heated to 40°C, and samples cooled to 20°C after heating at 40°C)

(b) A decrease in the mechanical performance of PCM–mortars was observed when the PCM state changed from solid to liquid when the sample was placed in the oven. The degree of strength degradation due to the change of the PCM state increased with increasing PCM content**.**

(c) Mechanical tests performed on PCM–mortar samples re-cooled to 20°C after having been heated in a 40°C oven for 6 h indicate that the mechanical strengths of the PCM–mortar samples were not totally recoverable**.**

(d) The degree of strength recovery of re-cooled PCM–mortar samples (samples cooled to 20 °C after heating at 40°C) decreased with the increase of PCM content**.**

(e) Bending strength exhibits a lower rate of recovery compared to compression strength.

(f) In the same trend of the compression and flexural behaviour, the stiffness of the PCM-mortar is not totally recoverable.

3-1-2 Explanation of the effect of temperature on the mechanical behaviour of the PCM-mortar matrix.

Figure 5 shows the evolution of the longitudinal strain and surface temperature versus time in the oven for the 15 and 20wt% PCM–mortar samples.

The 15 and 20wt% PCM–mortar samples exhibited an increase in the strain, which began in the range 24–25°C; this corresponds to the phase change of PCM from the solid state to the liquid state. No strain variation was observed in the range 15–23°C (all PCM in the mortar is in the solid state) or in the range 34–40°C (all PCM in the mortar has melted and is in the liquid state). In the temperature range 25–34°C, the PCM melts gradually from the surface to the internal volume of the sample.

Correspondingly, analysis of the change of the samples surface temperature as a function of time spent in the oven shows a constant rate of temperature increase until 24–25°C, where a slowdown in the temperature increase is observed. This is explained by the fact that at 24–25°C, PCM absorbs heat from the oven (in the form of latent heat) to undergo phase change, which causes a decrease in the rate of temperature increase. After the phase change, the rate of temperature increase raises in the 15 and 20wt% PCM-mortar samples (**Figure 5 a and b**).

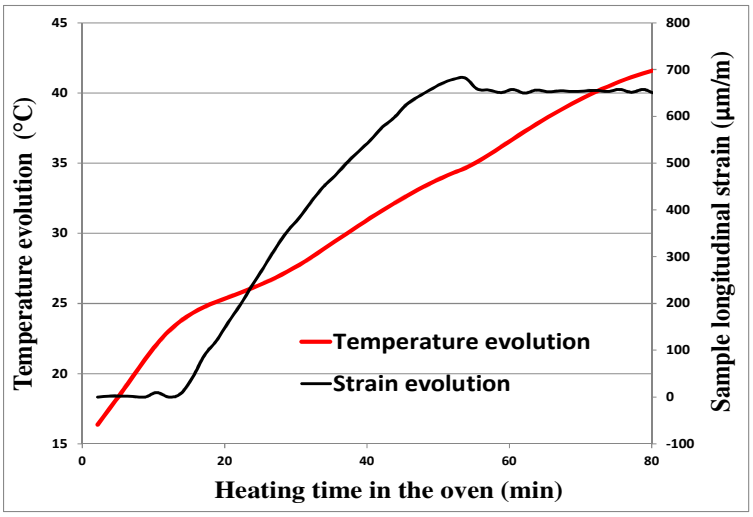

-a- 15wt% PCM-mortar

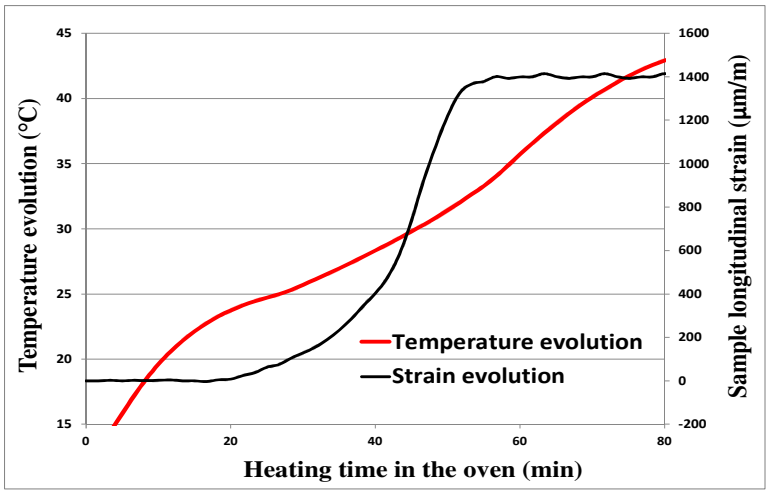

-b- 20wt% PCM-mortar

Figure 5 Evolution of strain and temperature for (a) 15wt % and (b) 20wt %PCM-mortars

Figure 6 shows the evolution of the longitudinal strains of all the PCM-mortar samples as a function of the surface temperature. It can be seen that the induced strains increase with increasing PCM content in the PCM-mortar matrices. The internal strain ε caused by the PCM expansion and the yield strain under direct tensile loading (experimentally evaluated for each PCM-mortar matrix) are summarised in **Table 3**.

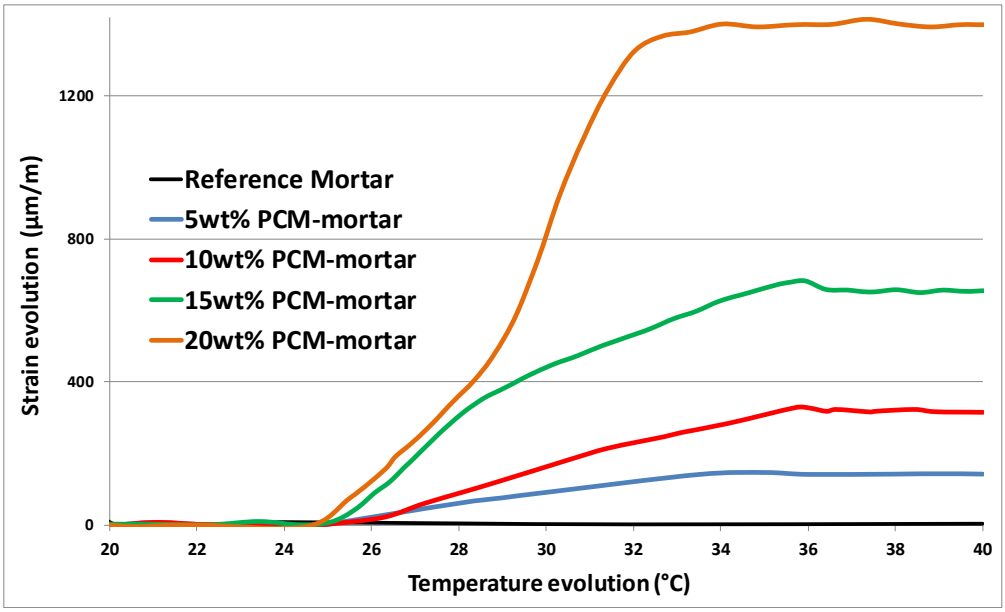

Figure 6 Evolution of longitudinal strain versus temperature for PCM-mortar samples

PCM-mortars	5wt %	10wt %	15wt %	20wt %
Induced strain (µm/m)	156± 9	306±20	650±45	1400±90
Yield strain (µm/m)	146±8	167±12	210 ±17	247 ±25

Table 3 Strains induced in PCM-mortar samples by PCM phase change

It can be concluded from **Table 3** that the volume change of the PCM during melting can induce multicracking in the mortar (induced strain due to PCM expansion > yield strain), which explains the significant degradation of the mechanical performances of the matrix during the tests at temperatures above 40°C (see **Section 3-1**). The number of formed cracks increases with increasing PCM content; therefore, the degradation of the mechanical performance of matrices becomes more significant with increasing PCM content. The partial recovery of the initial mechanical properties of the PCM-mortar matrices when the PCM re-solidifies is attributed to the partial closure of crack lips (caused by volume contraction) and a strength gain due to PCM solidification. The bending strength being more controlled by the presence of microcracking in the matrices exhibits a rate of recovery less important than the compressive strength (see **Figure 4**).

3-1-3 Mechanical characterisation of PCM-TRC composites

3-1-3-1 Mechanicals tests at variable PCM rate and constant temperature

The results obtained during the tensile tests on the PCM-TRC composites at different PCM rates (0, 5, 10, 15, and 20wt%) were analysed to determine their average macroscopic constitutive law in terms of stress versus strain, as presented in **Figure 7.**

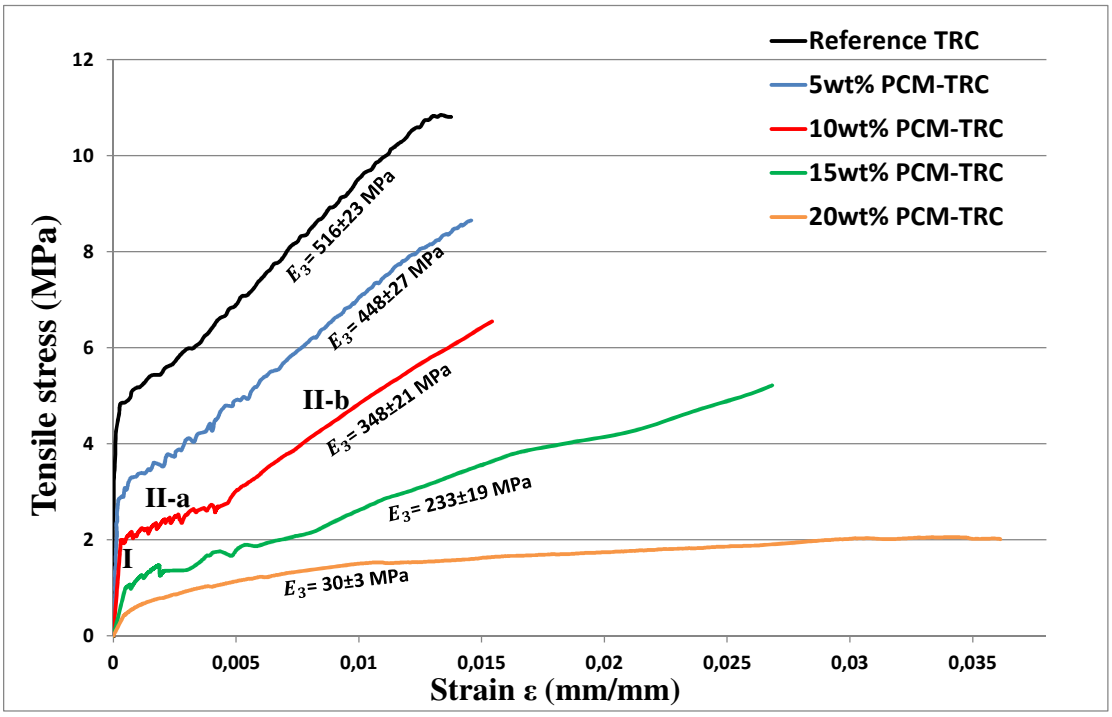

Figure 7 Stress versus strain behaviour of PCM-TRC composites during tensile test at T=20°C

Table 4 presents the evolution of main PCM-TRC characteristics according to PCM rate.

PCM-TRC	E_1(GPa)	σ_{BMC} (MPa)	E_3(MPa)	σ_{CF}(MPa)
Reference	31.2 ±1.2	4.15±0.18	516±23	10.85±0.5
5wt% PCM-TRC	20.1 ±0.8	2.92±0.13	448±27	8.64± 0.51
10wt% PCM-TRC	12 ±0.5	2.0±0.09	348±21	6.54± 0.4
15wt% PCM-TRC	5 ±0.2	1.05±0.05	233±19	5.17± 0.41
20wt% PCM-TRC	2.1±0.1	0.52±0.02	30±3	2.02± 0.21

E_1: modulus of PCM-mortar matrix, E_3: stiffness modulus of PCM-TRC in phase II-b

σ_{BMC}: stress at the initiation of multicracking, σ_{CF} : stress at composite failure

Table 4 Evolution of PCM-TRC characteristics during the tensile test

The global behaviour of the PCM-TRC composite (for all PCM rates) can be summarised as follows:

Phase I (see **Figure 7**) corresponds to a perfectly linear evolution governed by the mechanical properties of the matrix up to the initiation of the first macrocrack. During **phase II-a** (see **Figure 7**), the elastic limit of the matrix is reached progressively along the length of the composite, and each time a crack is created, the force is transmitted progressively from the matrix towards the textile at the location of the crack. **In phase II-b** (see **Figure 7**) the textile recovers almost all the tractive effort and the stiffness modulus of the composite (**E_3; see Table 4**) is governed by the elastic modulus of the reinforcing textile and its rate of work.

The first finding obtained by analysing the stress versus strain curves is that the strain hardening behaviour (ductile behaviour) and the matrix/textile charge transfer kinetics are maintained in the presence of microencapsulated PCM in TRC. However, it can be seen that the tensile strength of the PCM-TRC composites decreases when increasing the PCM rate.

By analysing in more detail the stress versus strain curves, one can note that:

In phase I, the stress at the onset of the initial cracking, which corresponds to the elastic limit of the PCM–mortar matrix, decreases with increasing PCM rate. This is explained by the fact that the addition of PCM in the mortar weakens its mechanical performance. Similarly, the elastic modulus in phase I decreases with decreasing PCM content owing to the weakening of the rigidity of the matrix.

The multicracking phase (**phase II-a**) is clearly visible in the majority of PCM-TRC composites; however no particular conclusion can be drawn as to the effect of the PCM rate on this phase.

During **phase II-b**, the load is almost entirely transmitted to the textile reinforcement. It can be seen after calculation (see **Table 4**) that the stiffness modulus of the composite (**E_3, during phase II-b, see Figure 7**) decreases with increasing PCM content. The rigidity modulus E_3 of the PCM-TRC composite in **phase II-b is a direct indicator** of the textile efficiency (textile rate of work) inside the PCM-TRC composite.

It can also be seen in **phase II-b** that the strain at failure of the composites is almost constant up to the level of 15% PCM, where an increase of the strain at rupture is observed. This is explained by the fact that for the 0, 5, and 10wt% PCM-TRC samples, the mode of failure was rupture of the textile under tension, whereas for the 15 and 20wt% PCM-TRC samples, rupture occurred by delamination of the textile layers due to the weakening of the shear strength of the interlaminar layer by the addition of PCM (see **Figure 8**). Indeed, the LVDT sensors positioned on the faces of the 15 and 20wt% PCM-TRC samples measured a parasitic displacement due to interlaminar slip upon the occurrence of shear delamination, which explains the large increases of the strain at failure for the 15 and 20% PCM-TRC samples in comparison with the 0, 5, and 10wt% PCM-TRC composites.

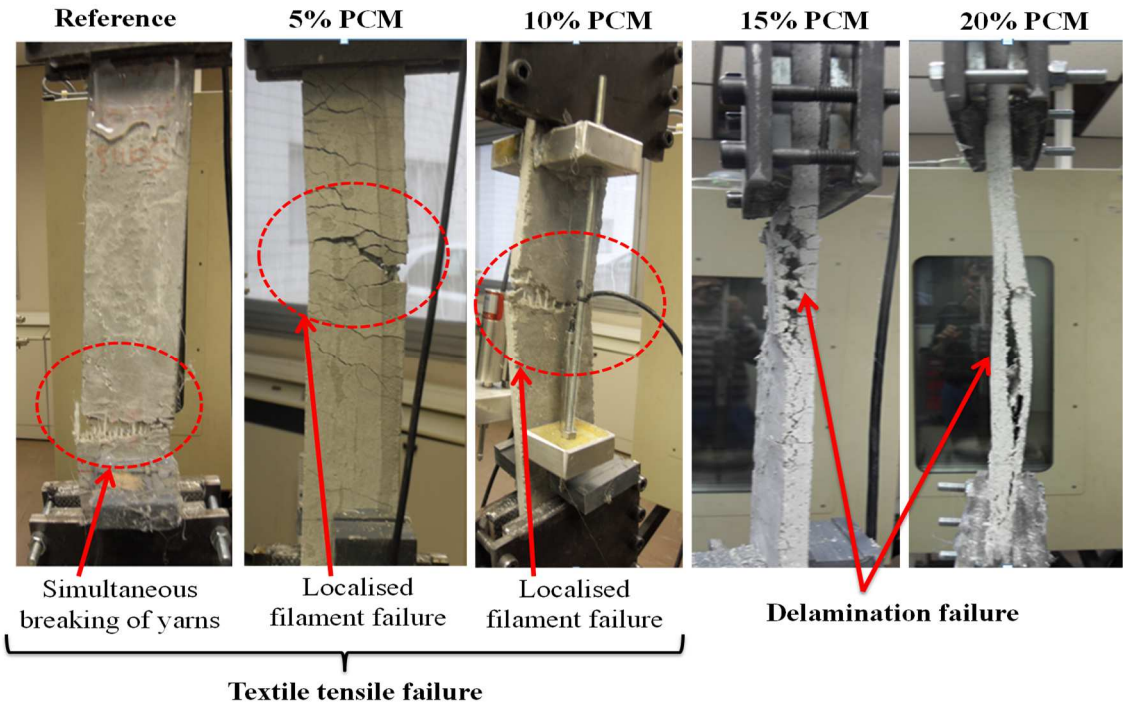

Figure 8 Failure modes of PCM-TRC composites

It should also be emphasised that even though a similar textile rupture mode occurred up to a PCM rate of 10wt%, a clear distinction exists between the failure mode of the reference composite (without PCM), where a simultaneous failure of the textile yarns occurred, and the 5 and 10wt% PCM-TRC composites, where localised filament breaks (which initiate the failure of the textile fabric) are observed **(see Figure 8 above)**. This is explained by the heterogeneous distribution of stresses in the textile yarns due to PCM addition in the 5 and 10wt% PCM-TRC composites. This phenomenon is explained in **Section 3-2-1-2.**

3-1-3-2 Mechanical tests at variable temperature and constant PCM rate

The average curves (stress versus strain for three samples) of the tensile behaviour of the 10wt% PCM-TRC composite held at 20°C and tested at the same temperature and for the 10wt% PCM-TRC composite heated at 40°C for 6 h (to induce PCM phase change) are presented in **Figure 9**.

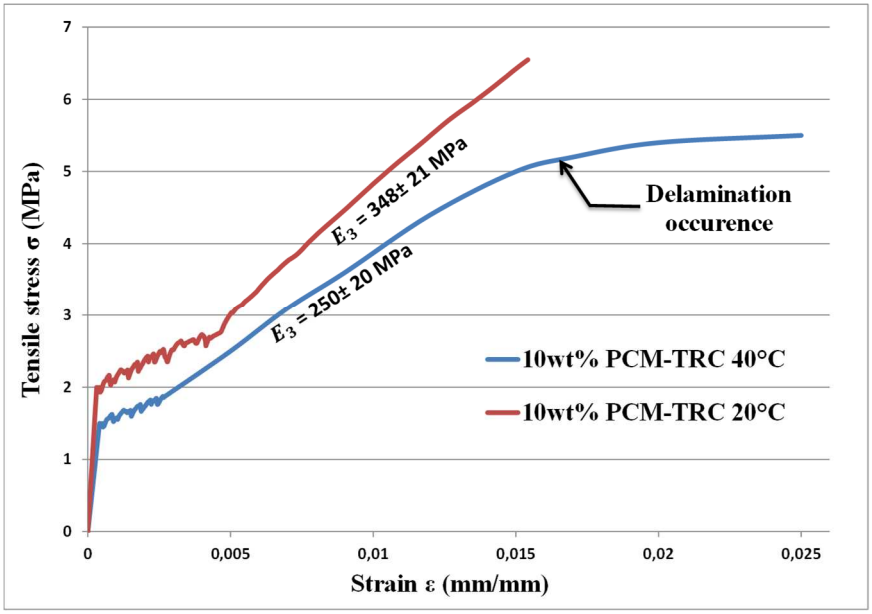

Figure 9 Effect of PCM phase change on the mechanical behaviour of 10% PCM-TRC

From **Figure 9**, it can be seen that the 10wt% PCM-TRC composite heated at 40°C has a 20% lower resistance than the sample held at 20°C.

By analysing in more detail:

In **phase I**, the 10wt% PCM-TRC composite heated at 40°C exhibits a decrease of 25% in stress at the onset of cracking (σ_{BMC}) and a decrease of 33% in the elastic modulus of the matrix (E_1) in comparison with the composite maintained at 20 °C **(Figure 9).** This is explained by the degradation of the mechanical performance of the matrix by the creation of internal microcracks at temperatures higher than the melting temperature of PCM (see **Section 3-1-1**).

In **phase II-b**, the stiffness modulus E_3 of the 10wt% PCM-TRC composite heated at 40 °C shows a decrease of ~30% compared with the composite maintained at 20°C (**see Figure 9**). This is explained by a degradation of the intensity of the matrix/textile interaction due to the creation of internal microcracks in the interface. In fact, the creation of microcracks at the matrix/textile interface can reduce the effective contribution of the textile owing to the degradation of the kinetics of charge transfer from the matrix to the cracked interface to the textile. This trend is

confirmed by analysing the failure mode of the 10wt% PCM-TRC sample heated to 40°C. In fact, the rupture of that sample occurred by delamination between layers of reinforcement (see **Figure 10**) due to the degradation of the shear strength of the interlaminar layer by cracking during placement in the oven. Meanwhile, we can observe that the rupture of the 10wt% PCM-TRC composite maintained at 20°C occurred by textile breaking under tension (see **Figure 10**).

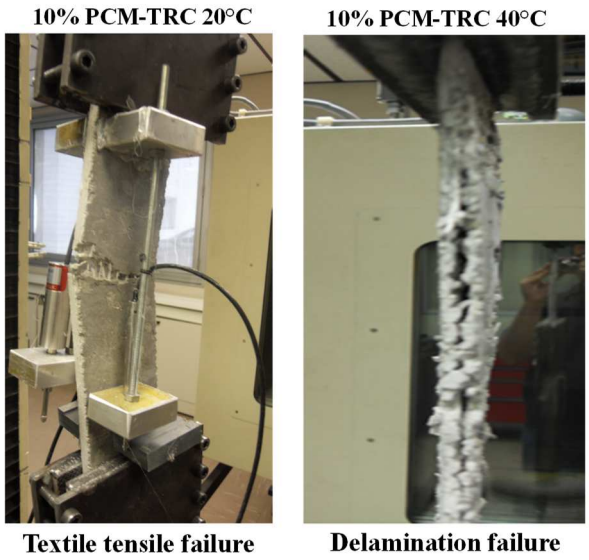

Figure 10 Effect of PCM phase change on the failure mode of the 10wt% PCM-TRC sample

The increase of the strain at failure for the 10wt% PCM-TRC composite heated at 40°C is due to its characteristic failure mode by delamination. Indeed, an interlaminar slip was detected by the displacement transducers, which explains the increase of the strain at failure while the transmitted stress is almost constant.

3-2 Physico-chemical characterisation of the PCM-TRC composites

3-2-1 SEM observations

3-2-1-1 SEM observations in the control TRC composite (without PCM)

Figure 11 shows an SEM image representative of a longitudinal cross-section at the "matrix /textile" interface in a reference TRC composite (without PCM).

It can be seen from **Figure 11** that a very low porosity remains at the transition zone between the reference mortar matrix (without PCM) and the textile; therefore, high stiffness can be achieved in the characteristic **zone II-b** of the stress–strain plot of TRC under tension (see **Figure 7, reference TRC**) in the reference TRC composite (without PCM).

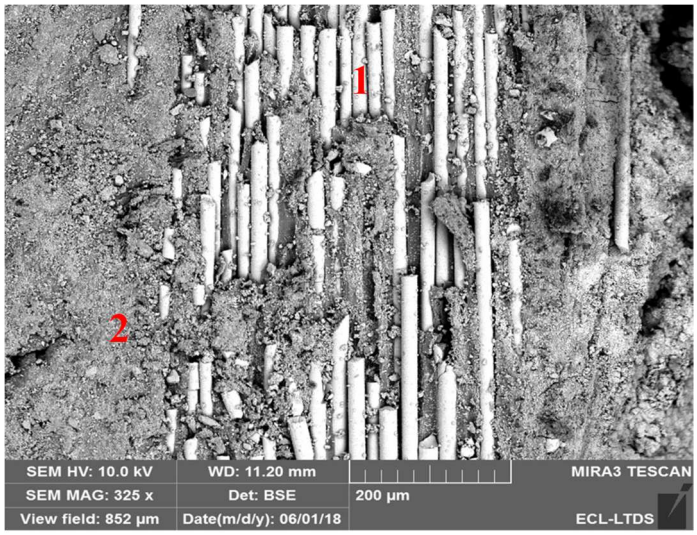

Legend: 1 Textile, 2 Reference matrix

Figure 11 SEM image of the reference TRC composite (without PCM)

The very low porosity at the interface also allows a homogeneous distribution of stresses between the external textile filaments, which are in direct contact with the matrix. This explains the simultaneous failure of the textile yarns during the tensile test on the reference TRC specimens (see **Section 3-1-3-1**)

3-2-1-2 SEM observations in the PCM-TRC composites

3-2-1-2-a PCM-particles identification

Figure 12, which was obtained by the BSE detector**,** shows the microstructure of a small amount of PCM powder sheared between two pieces of glass. Manual shearing allows distinguishing intact PCM particles from damaged ones.

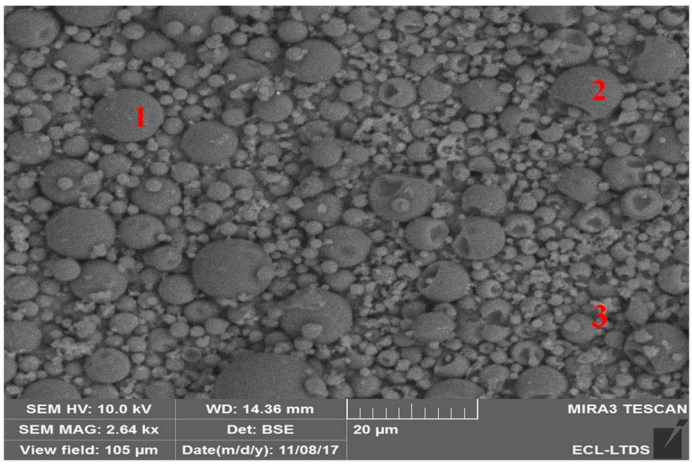

Legend:1 Unbroken capsules , 2 Damaged PCM capsules, 3 Pure PCM wax

Figure 12 SEM observation of PCM powder with damaged and undamaged capsules

It can be seen that the broken PCM particles contains small nodules, which represents the pure PCM wax. BSE detector distinguishes PCM wax (small nodules) from undamaged PCM capsules owing to the higher density of the former.

3-2-1-2-b Effect of PCM on the matrix hydration in the vicinity of the interface

Figure 13 presents an SEM image of a 15wt% PCM-TRC composite. The objective here is to determine the effect of PCM on the hydration of cement near the matrix/textile interface.

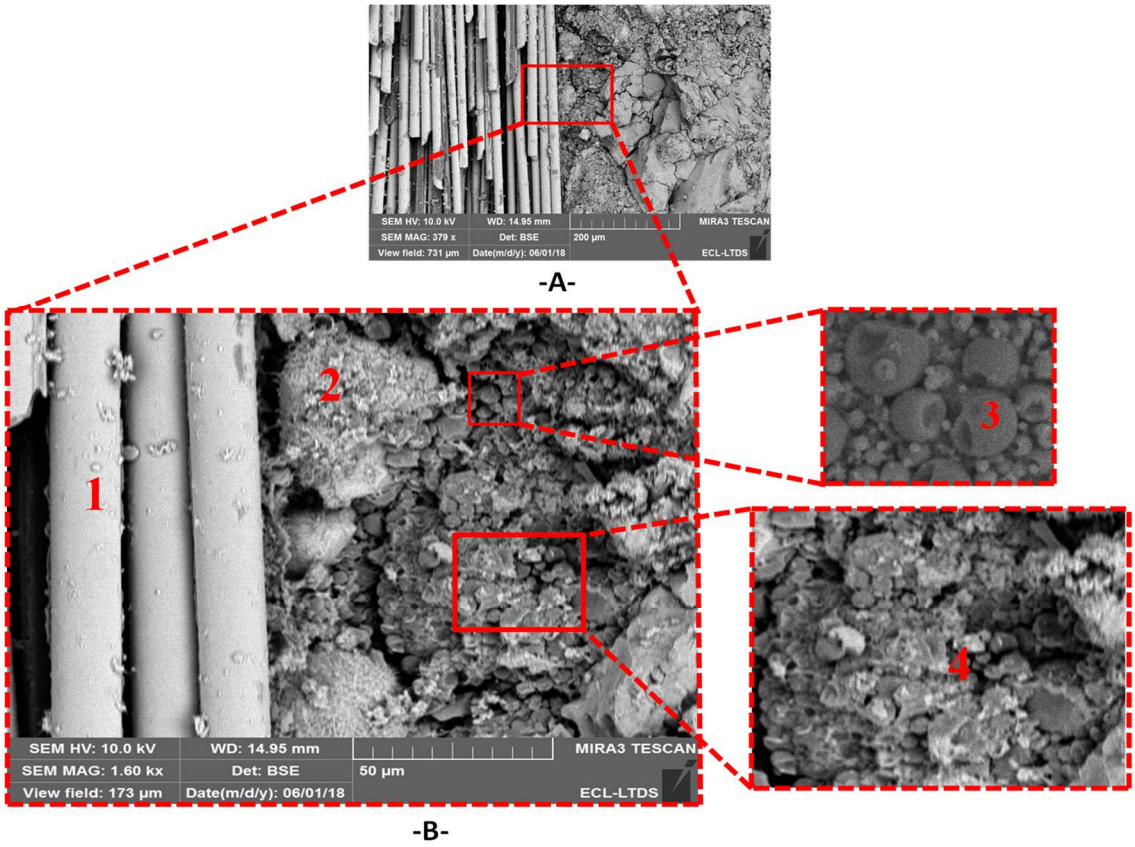

Legend : 1 Textile, 2 Cement, 3 PCM microcapsule, 4 Agglomeration of PCM particles

Figure 13 SEM image illustrating the effect of PCM on cement hydration near the interface

From **Figure 13**, it can be seen that the long chain of PCM capsules surrounding the anhydrous cement grains in the matrix/textile interface zone can limit or even prevent their hydration by restricting their access to water and thus their dissolution. This reduces the amount of hydrated products from the cement in the matrix/textile interface zone and therefore limits the contribution of the textile reinforcement to recover the tractive effort. This trend of PCM to inhibit the hydration of cement was confirmed by semi-adiabatic calorimetry realised by the authors in [12] on PCM-mortar matrix with different PCM rates.

3-2-1-2-c Effect of PCM damage in the vicinity of the interface

Figure 14 shows another SEM image presenting a longitudinal cross-section at the matrix/textile interface in a 10wt% PCM-TRC composite. The purpose of this figure is to highlight the effect of the deposition of pure PCM wax in the matrix/textile interface zone.

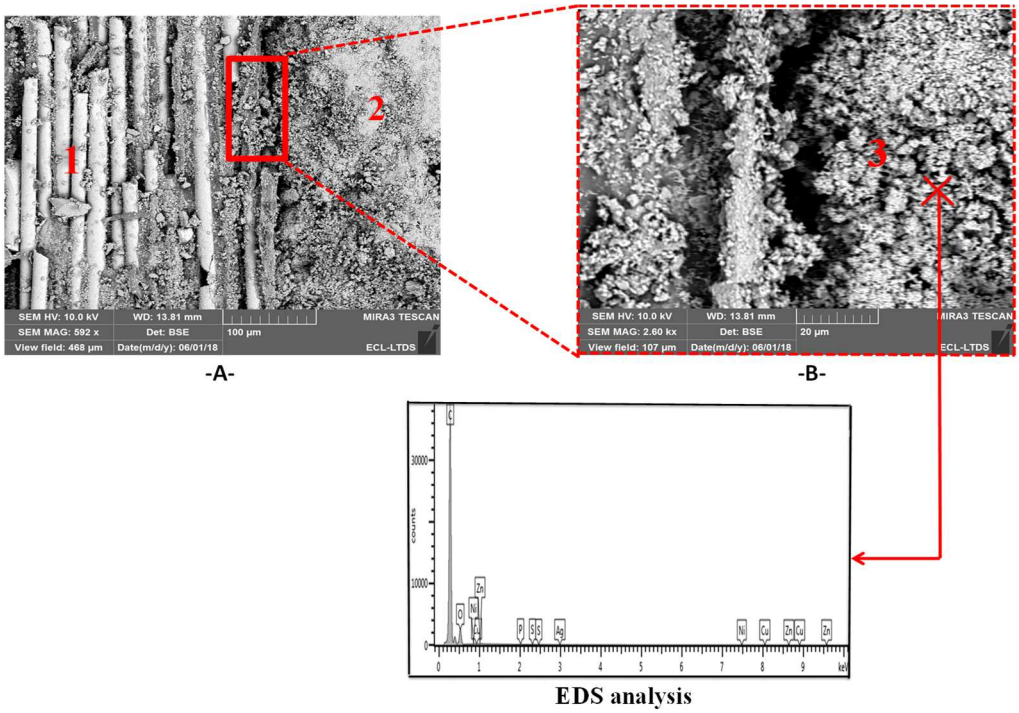

Legend : 1 Textile, 2 CSH hydrated product, 3 leaked PCM wax from damaged capsules

Figure 14 SEM image illustrating the effect of PCM wax leakage near the interface

Figure 14 clearly shows the existence of large quantities of pure PCM wax nodules resulting from the damage of PCM microcapsules (previously identified in the SEM analysis of the PCM microcapsules and visible in **the legend 3 of Figure 14**) in the matrix/textile interface zone. The presence of PCM wax is confirmed by the energy-dispersive X-ray spectroscopy analysis in the red highlighted zone in **Figure 14-B**. In fact, the intense carbon peak and the less pronounced oxygen peak are attributed to the pure PCM oil, which has a semi-developed chemical formulation of CH_3-CH_2(14)-C(O)-O-CH_2.

The deposition of a large quantity of pure PCM nodules in the direct vicinity of the matrix/textile interface shown in **Figure 14** is most likely due to the damage of PCM microcapsules during the application of the hand lay-up technique to the PCM-TRC composite and/or during the mixing procedure. The immiscibility of pure PCM wax in water also inhibits the hydration of the cement and promotes the formation of porosity in the vicinity of the interface. It can clearly be seen in **Figure 14-A** that the progression of the CSH gel growth (**CSH gel is visible in legend 2 of Figure 14**) is inhibited in the deposition zone of the leaked pure PCM oil in the direct vicinity of the matrix/textile interface.

3-2-1-2-d Effect of macrospores in the vicinity of the interface

Figure 15 shows another SEM image of a 15wt% PCM-TRC composite. The figure shows the existence of macrospores (cavities, macro air bubble) near the 'matrix/textile' interface. These macro cavities are attributed to the presence of PCM agglomerate, which is favoured by the presence of pure PCM wax (PCM nodules) acting as an adhesive between PCM capsules, increasing the viscosity of the pore media and inducing porosity. These macro air bubbles contribute to the global degradation of the 'matrix/textile' interaction efficiency.

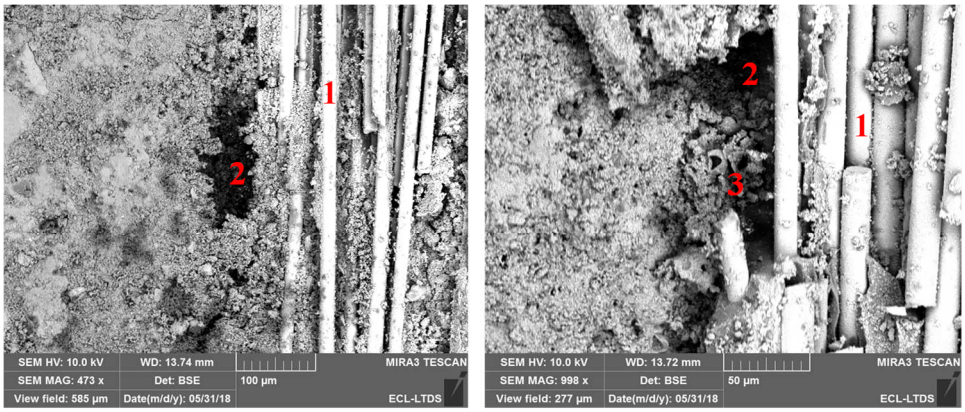

Legend : 1 Textile, 2 Macropores (cavity), 3 PCM agglomeration

Figure 15 SEM observations illustrating the existence of macrospores near the interface

The phenomena discussed above (**Section 3-2-1-2, b, c and d**) show that the loss of bond between mortar and textiles due to the reduced interface surface (**that can be a assessed in the different SEM images Section 3-2-1-2, b, c and d**) is one of the main reasons for the decrease of the textile rate of work when increasing PCM content.

The phenomena discussed above (**Section 3-2-1-2, b, c and d**) show also the variability of the PCM effects at the interface level that contributes in different ways to the alteration of the matrix/textile interaction intensity. This induces a disparity between the stress distributions of the textile yarns as the PCM level increases in the PCM-TRC composites. This phenomenon explains the localised filament failures in the 5 and 10wt% PCM-TRC samples, while a more homogeneous and almost simultaneous rupture of the textile yarns was found for the reference (without PCM) TRC composite (see **Section 3-1-3-1**).

Figure 16 illustrates a qualitative scheme that explains in a simplified manner the distribution of normal stresses at the matrix/textile interface before and after the integration of PCM into the cement matrix. The figure shows the distribution disparity in the normal stresses on the circumferential filaments (external filaments) of the yarn due to the effect of PCM.

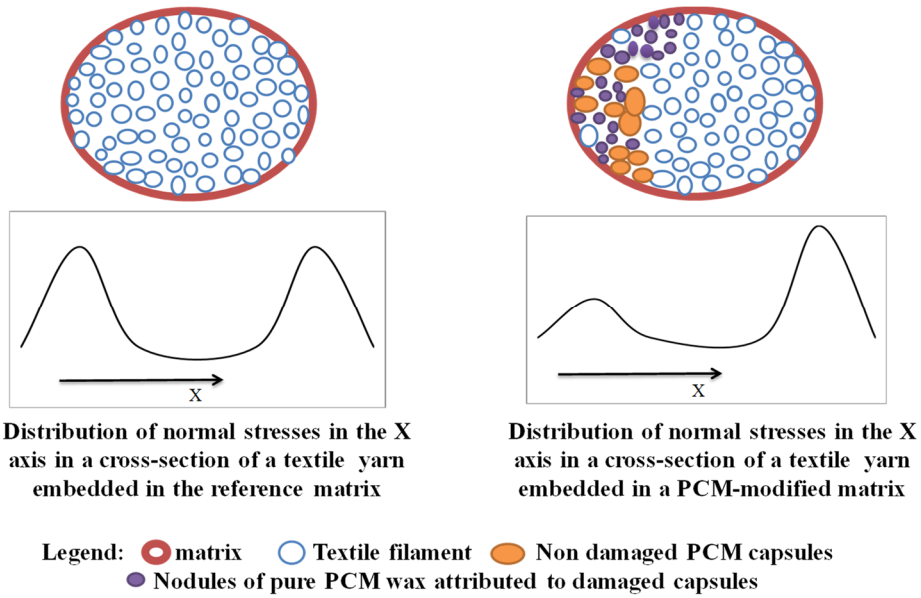

Figure 16 Distribution of stresses in a textile yarn section before and after integration of PCM

3-2-1-2-e Effect of PCM phase change in the vicinity of the interface

Figure 17 shows an SEM observation of a 15wt% PCM-TRC composite placed in an oven at 40°C for 6 h. The figure displays the occurrence of multicracking at the matrix/textile interface (attributed to the volume expansion of PCM due to its phase change from solid to liquid), which explains the degradation of the charge transfer at the matrix/textile interface due to the effect of the temperature, as discussed in **Section 3-1-2**

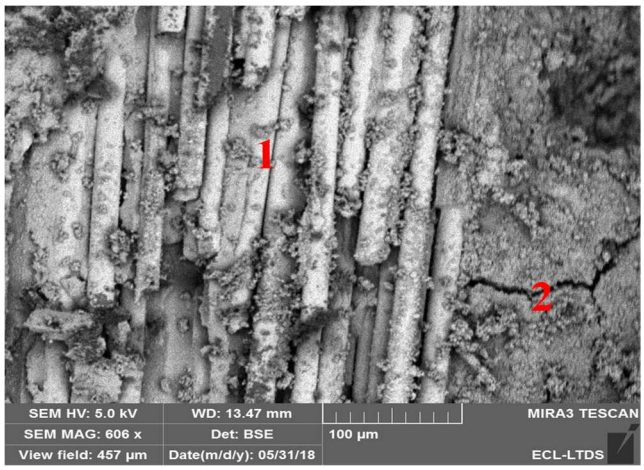

Figure 17 SEM observation showing the effect of PCM phase change near the interface

3-2-2 DSC analysis

The evolution of the specific heat measured by the CALVET calorimeter for the 0, 5, 10, 15, and 20wt% PCM-TRC composites as a function of the temperature is presented in **Figure 18**.

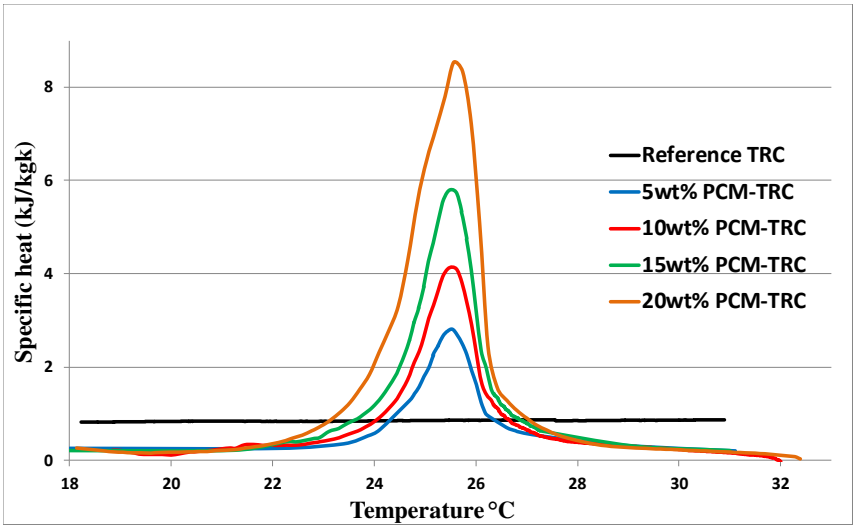

Figure 18 Evolution of PCM-TRC heat capacity during an endothermic cycle

The DSC analysis demonstrates that PCM significantly increases the thermal capacity of PCM-TRC.

The evaluated performance factor T_{the} (equation 1), defined as the ratio of the heat stored during an endothermic cycle and the theoretical storable heat Q_{the}, is given in **Table 5**.

$$T_{the} = \frac{\int_5^{40} m \times Cp_{PCM-mortar}\, dT}{Q_{the}} \quad (1)$$

Where Q_{the} is evaluated by the homogenisation law:

$$Q_{the} = \int_5^{40} [\eta_{PCM}\, Cp_{PCM} + \eta_{mortar} Cp_{mortar}] \quad (2)$$

η_{PCM} and η_{mortar} are the massic rates of the PCM and mortar, respectively.

PCM-TRC	5wt% PCM-TRC	10wt% PCM-TRC	15wt% PCM-TRC	20wt% PCM-TRC
T_{the}	94.27±2.82	98.58±3.54	102.65±3.79	97.62±3.41

Table 5 Thermal performance factor of PCM-TRC composites

From **Table 5** it can be seen that the performance factors are close to 100% with a slight uncertainty due to the relative error in the PCM rates. It can therefore be concluded that the thermal performances of the PCM-TRC composites are roughly conserved despite the damage observed in some PCM microcapsules.

3-Conclusion

This paper focuses on the mechanical and physicochemical characterisation of new PCM-TRC composites derived from the association of a non-paraffinic encapsulated PCM modified cementitious matrix and textile reinforcement.

On the basis of the experimental investigations presented above, the following conclusions can be drawn:

A/ At the matrix scale

1. The addition of encapsulated PCM to the mortar results in a significant reduction in its resistance.

2. A decrease in the mechanical performance of the PCM–mortars is observed when the PCM state changes from the solid to the liquid state. The inability of PCM–mortar matrices to recover all of their initial mechanical strengths upon re-solidification of the PCM is due to microcracks induced by the expansion of the microcapsules during the phase change.

B/ At the composite scale

1. The ductile mechanical behaviour and the matrix/textile charge transfer kinetics in the TRC composites are maintained in the presence of microencapsulated PCM.

2. The mechanical performances of the PCM-TRC composites degrade with increasing PCM content; furthermore, a critical failure mode by delamination between layers of reinforcement is detected for PCM content around 15wt%.

3. A decrease of the textile rate of work is observed when increasing the PCM content in the PCM-TRC composites. This is due to the disorder caused by the PCM in the matrix/textile interface area, as revealed by SEM observations. Specifically:

- The agglomeration of PCM capsules surrounding the anhydrous cement grains in the matrix/textile interface zone. This agglomeration limits or even prevents the hydration of cement grains by restricting their access to water and thus their dissolution. This reduces the amount of hydrated products from the cement in the matrix/textile interface zone and consequently limits the contribution of the textile reinforcement to the recovery of tractive efforts.
- The deposition of pure PCM wax in the direct vicinity of the matrix/textile interface zone due to the damage of the PCM microcapsules during the hand lay-up and/or mixing procedures, which inhibits the progression of hydrates and thereby promotes pore formation in the interface zone.
- The formation of macrospores (cavities) due to the presence of PCM agglomerates in the interface zone, which contributes to the degradation of the matrix/textile interaction efficiency.

4. The temperature has an effect on the mechanical behaviour of the PCM-TRC composites. A drop of tensile strength and a decrease of the textile efficiency work are observed for the 10wt% PCM-TRC composite heated at 40°C in comparison with the composite maintained at 20°C. This is due to the degradation of the matrix/textile interface caused by multicracking, which is due to PCM expansion during its phase change from solid to liquid.

5. A proportion of the PCM microcapsules break during the mixing process and/or the hand lay-up process of the composites. However, DSC analysis reveal that the thermal energy storage of PCM-TRC composites is not affected.

Acknowledgement

The authors thanks KAST company (Sonthofen, Germany) for providing the textile reinforcement used in the study

Funding:

The Academic research community (ARC ENERGIES and SCUSI) of the Rhone-Alpes and Auvergne FRANCE region funded this study

The authors declare that they have no conflicts of interests.

Bibliography

[1] T D'Antino, C Papanicolaou, Mechanical characterization of textile reinforced inorganic-matrix composites, Composites Part B 127 (2017) 78-91

[2] Z Djamai, M Bahrar, F Salvatore, A Si Larbi, M El Mankibi, Textile reinforced concrete multiscale mechanical modelling: Application to TRC sandwich panels, Finite Elements in Analysis and Design 135 (2017) 21-35

[3] J Vervloet, P Van Iterbeek, S Verbruggen, M El Kadi, M De Munck, J Wastiels,T Tysmans, Experimental investigation of the buckling behaviour of Textile Reinforced Cement sandwich panels with varying face thickness using Digital Image Correlation, Construction and building materials, 51 (2014) 405-413

[4] A Shams, J Hegger, M Horstmann, An analytical model for sandwich panels made of textile reinforced concrete, Construction and Building Materials 64 (2014) 451-459

[5] I Colombo, M Colombo, M Di Prisco, Bending behavior of textile reinforced concrete sandwich beams, Construction and Building Materials 95 (2015) 675–685.

[6] Z I Djamai, K Erroussafi, A Si Larbi, F Salvatore, G Cai Analytical modeling of textile reinforced concrete (TRC) sandwich panels: Consideration of nonlinear behavior and failure modes, Mechanics of advanced Materials and structures (2020).

[7] M Pomnianowski, P heiselberg, R Jensen, R Cheng, Y Zhang, A new experimental method to determine specific heat capacity of inhomogeneous concrete material with incorporated microencapsulated –PCM, Cement and concrete research 55 (2014) 22-34.

[8] H W Min, S Kim, H S Kim, Investigation on thermal and mechanical characteristics of concrete mixed with shape stabilized phase change material for mix design, Construction and building materials 149 (2017) 749-762.

[9] A Figueiredo, J Lapa, R Vicente, C Cardoso, Mechanical and thermal characterization of concrete with incorporation of microencapsulated PCM for applications in thermally activated slabs in Construction and Building Materials (2016) 126 332-344.

[10] S Cunha, M Lima, J Aguiar, Influence of adding phase change materials on the physical and mechanical properties of cement mortars, Construction and Building Materials 127 (2016) 1–10

[11] D Zhang, Z Li, J Zhou, K Wu, Development of thermal energy storage concrete, Cement and Concrete Research 34 (2004) 927-934

[12] Z Djamai, F Salvatore, A Si Larbi, G Cai, M El Mankibi, Multiphysics analysis of effects of encapsulated phase change materials (PCMs) in cement mortars, Cement and Concrete Research 119 (2019) 51-63.

[13] A Eddhahak-ouni, S Drissi, J colin, J Negi, S Carre, Experimental and multi-scale analysis of the thermal properties of Portland cement concretes embedded with microencapsulated phase change materials (PCMs), Applied thermal engineering 64 (2014) 32-39.

[14] V D Cao, S Pilehvar, C Salas-Bringas, A M Szczotok, Microencapsulated phase change materials for enhancing the thermal performance of Portland cement concrete and geopolymer concrete for passive building applications, Energy Conversion and Management 133 (2017) 56-66.

[15] A Thiele, A Jamet, G Sant, L Pilon, Annual energy analysis of concrete containing phase change materials for building envelopes in Energy conversion and management 103 (2015) 374-386.

[16] M Aguayo, S Das, A Maroli, N Kabay, J Mertens, S Rajan, G Sant, N. Chawla, N. Neithalath, The influence of microencapsulated (PCM) characteristics on the microstructure and strength of cementitious composites: Experiments and finite element simulations, Cement and Concrete Composites 73 (2016) 29-41

[17] P K Dehdezi, M R Hall, A R Dawson, S P Casey, Thermal, mechanical and microstructural analysis of concrete containing microencapsulated phase change materials, Int. J. Pavement Eng. 14 (5) (2013) 449–462.

[18] H Cui, W Liao, X Mi, T Lo D Chen, Study on functional and mechanical properties of cement mortar with graphite-modified microencapsulated phase-change materials, Energy and Building 105 (2015) 273-284

[19] T Lecompte, P Le Bideau, P Glouannec, D Nortershausser, S Le masson, Mechanical and thermos-physical behaviour of concretes and mortars containing PCM, Energy and Buildings 94 (2015) 52-60.

[20] M Hunger, A G Entrop, I Mandilaras, H J H Brookers, M Founti, The behavior of self-compacting concrete containing micro-encapsulated phase change Materials, Cement and Concrete Composites 31 (2009) 731–743

[21] B Savija, M Lukovic, G Kotteman, S Figueredo, F de Mendoça Filho, E Schlangen Development of ductile cementitious composites incorporating microencapsulated phase change materials, International Journal of Advanced science and Applied Mathematics 9 (2017) 169-180

[22] S Pilehvara, V-D Cao, A M Szczotoka, L Valentinie Mechanical properties and microscale changes of geopolymer concrete and Portland cement concrete containing micro-encapsulated phase change materials, Cement and Concrete Research 100 (2017) 341-349

[23] A de Gracia, L Rincon, A Castell, M Jimenez, D Boer, M Medrano, L F Cabeza Life cycle assessment of the inclusion of phase change materials in experimental building, Energy and Buildings 42 (2010) 1517-1523.

[24] C Castellón, A Castell, M Medrano, I Martorell, L F.Cabeza Experimental Study of PCM Inclusion in Different Building Envelopes, Journal of Solar Energy Engineering 131(2009) 1-6

[25] S Cunha**,** J Aguiar, V Ferreira, A Tadeu, A Garbacz Mortars with phase change materials - Part I: Physical and mechanical characterization*, Key* Engineering Materials 634 (2015) 22-32

[26] M Felix, J Aguiar Study of a cement mortar with incorporation of PCM microcapsules in proceeding of the 6th symposium of polymers in concrete, Shanghai China

[27] Tests for mechanical and physical properties of aggregates Part 6: Determination of particle density and water absorption

[28] RILEM Technical Committee Recommendation 232-TDT: test methods and design of TRC Materials and structures (2016) 4923-4927